



Universiteit  
Leiden  
The Netherlands

## **Solid state $^{13}\text{C}$ NMR spectroscopy on EPDM/PP/oil based thermoplastic vulcanizates in the melt**

Winters, R.; Lugtenburg, J.; Litvinov, V.M.; Duin, M. van; Groot, H.J.M. de

### **Citation**

Winters, R., Lugtenburg, J., Litvinov, V. M., Duin, M. van, & Groot, H. J. M. de. (2001). Solid state  $^{13}\text{C}$  NMR spectroscopy on EPDM/PP/oil based thermoplastic vulcanizates in the melt. *Polymer*, 42(24), 9745-9752. doi:10.1016/S0032-3861(01)00504-3

Version: Publisher's Version

License: [Licensed under Article 25fa Copyright Act/Law \(Amendment Taverne\)](#)

Downloaded from: <https://hdl.handle.net/1887/3239461>

**Note:** To cite this publication please use the final published version (if applicable).

# Solid state $^{13}\text{C}$ NMR spectroscopy on EPDM/PP/oil based thermoplastic vulcanizates in the melt

R. Winters<sup>a</sup>, J. Lugtenburg<sup>a</sup>, V.M. Litvinov<sup>b</sup>, M. van Duin<sup>b</sup>, H.J.M. de Groot<sup>a,\*</sup>

<sup>a</sup>Leiden Institute of Chemistry, Gorlaeus Laboratories, Leiden University, P.O. Box 9502, 2300 RA Leiden, The Netherlands

<sup>b</sup>DSM Research, P.O. Box 18, 6160 MD Geleen, The Netherlands

Received 21 September 2000; received in revised form 10 April 2001; accepted 2 July 2001

## Abstract

$^{13}\text{C}$  NMR and EPR methods are employed to quantitatively determine the composition of thermoplastic vulcanizates (TPVs) based on ethylene-propylene-diene rubber (EPDM), polypropylene (PP) and extender oil, with and without talcum filler. The oil has a strong influence on both the processing and the mechanical properties of TPVs, and the specific aim of this study is to determine the location of the oil in the melt.  $^{13}\text{C}$  NMR of the pure oil reveals that it closely resembles a low molecular weight EPM with  $\bar{M}_n = 800$  g/mol and an ethylene content of 70 wt%. EPR shows that traces of paramagnetic  $\text{Mn}^{2+}$  ions are present in the talcum filler. The  $\text{Mn}^{2+}$  ions appear to suppress a substantial fraction of  $\sim 30\%$  of the oil  $^{13}\text{C}$  NMR response. In contrast, the paramagnetic ions do not significantly affect the PP/EPDM ratio. Taken together, the NMR and EPR results provide strong evidence that in the melt about one third of the oil is neither mixed with EPDM nor PP. The data indicate that it may form a thin layer of  $\sim 0.05$   $\mu\text{m}$  characteristic thickness around talcum filler particles. © 2001 Elsevier Science Ltd. All rights reserved.

**Keywords:** Thermoplastic elastomer; NMR; Miscibility

## 1. Introduction

Thermoplastic elastomers (TPEs) are polymer materials that combine the processing characteristics of thermoplastics with the elastic and mechanical properties of vulcanized rubbers. An important class of TPEs is the thermoplastic vulcanizates (TPVs). Currently, TPVs comprise the fastest growing rubber market. TPVs are produced by dynamic vulcanization of blends containing a thermoplastic and an elastomer [1,2]. During preparation, the thermoplastic and the rubber are thoroughly mixed in the melt. The rubber phase is selectively crosslinked and forms a dispersion in the thermoplastic matrix. Commercial TPVs are generally made from isotactic polypropylene (PP), ethylene-propylene-diene rubber (EPDM) and extender oil. The rubber is crosslinked with an activated resol curing system [3]. Typical rubber particle sizes for such TPVs are 1–5  $\mu\text{m}$ . In addition, other additives such as fillers, for instance talcum or clay, stabilizers, pigments, etc. may be added.

The addition of oil in combination with crosslinking of the EPDM phase allows the production of soft compositions with good processability and elastic recovery. Very soft

TPVs are commercially available with 45 shore A hardness and compression sets approaching values normally encountered for thermoset rubbers, while the PP in the TPV allows good thermoplastic processing [4]. Upon cooling, the PP phase solidifies and partly crystallizes and the EPDM particles determine, to a large extent, the material properties in the solid state. In this rubbery state, the oil is generally believed to be predominantly absorbed by the EPDM phase [5]. Some oil can reside in the amorphous region of the PP phase, which improves the elasticity of the TPV [5]. Upon deformation, both the rubber particles and the thin PP layers surrounding the particles behave elastically [6,7], which explains the macroscopic elastic behavior. In the melt, the oil is probably distributed over both polymer phases. This yields a low viscosity and improves processability [8]. However, the distribution of the oil over the PP and EPDM phases at processing conditions has not yet been quantified. Such a determination is important for the rationale design of TPVs with optimal processability.

High-resolution solid state NMR spectroscopy is a powerful method for microscopic characterization of polymers. Detailed information about miscibility, intermolecular interactions, and morphology of polymer blends at or near the molecular level can be obtained by examining NMR parameters such as chemical shifts, line widths,

\* Corresponding author. Tel.: +31-71-274-539; fax: +31-71-274-537.

E-mail address: ssnmr@chem.leidenuniv.nl (H.J.M. de Groot).

Table 1  
Calculated compositions of TPVs

Recipe					NMR analysis			
	$m_{PP}$	$m_{EPDM}$	$m_{oil}$	$m_{PP}/m_{EPDM}$	$m_{PP}$	$m_{EPDM}$	$m_{oil}$	$m_{PP}/m_{EPDM}$
TPV-1 <sup>a</sup>	16.6	35.2	48.2	0.47	21.3±1.5	48.4±7.3	30.3±3.9	0.44±0.05
TPV-2	12.2	47.8	40.0	0.26	12.2±1.0	49.5±7.4	38.3±5.0	0.25±0.03
TPV-3 <sup>a</sup>	27.7	34.4	37.9	0.80	34.8±2.9	42.1±6.3	23.1±3.0	0.83±0.09
TPV-4	20.0	57.4	22.6	0.35	19.4±1.4	62.0±9.3	18.5±2.3	0.31±0.04

<sup>a</sup> TPV-1 and TPV-3 contain an additional amount of 10 wt% talcum.

relaxation parameters and polarization transfer processes [9–14]. These NMR parameters can help to locate the oil in the system.

In this work, NMR techniques are used in conjunction with EPR to determine the composition of the TPV and the location of the oil at processing temperatures. To achieve this, we first developed a method to quantify the composition of PP/EPDM/oil TPVs. Using this approach, the composition and distribution of the oil is investigated in four TPV systems with and without talcum filler.

## 2. Experimental

### 2.1. Preparation of TPVs

Four TPVs were prepared on a laboratory scale according to the recipes given in Table 1, by dynamic vulcanization of isotactic PP (DSM Stamylan<sup>®</sup> P, pentad mmmm > 93%), green strength ENB-containing EPDM (DSM Keltan<sup>®</sup>) and extender oil (Sunpar<sup>®</sup> 150). The material was crosslinked with up to 1.0 wt% (*p*-iso-octylphenol)-formaldehyde resin (resol; Schenectady<sup>®</sup> SP 1045) activated by stannous chloride (up to 0.50 wt%) and zinc oxide (up to 0.55 wt%). In two samples, TPV-1 and TPV-3, talcum (about 10 wt%) was added as a filler. In addition, a phenolic antioxidant was used as an additive. The TPVs were prepared either with a ZSK-30 extruder or with a 50 cm<sup>3</sup> Brabender mixer. Temperatures in the melt ranged from 200 to 260°C; the average residence time varied between 2 and 6 min.

### 2.2. NMR spectroscopy

Both solution and solid state <sup>13</sup>C NMR spectra were recorded at 100 MHz <sup>13</sup>C frequency with a Bruker MSL-400 spectrometer at temperatures between 20 and 180°C. For solution NMR, the materials were dissolved in 1,1,2,2-tetrachloroethane-*d*<sub>2</sub> (C<sub>2</sub>D<sub>2</sub>Cl<sub>4</sub>). Chemical shifts are given relative to TMS using the  $\delta = 74.1$  ppm signal from the natural abundance <sup>13</sup>C in the solvent as an internal standard. Solid state <sup>13</sup>C NMR spectra were collected from fragments of larger samples. The data were calibrated using the carboxyl resonance of glycine with  $\delta = 176.0$  ppm as an external reference. Spinning samples

were measured at room temperature in a 7 mm rotor using a spinning frequency of 4.5 kHz. The data were acquired with single pulse excitation and high power proton inverse gated decoupling. The 90° <sup>13</sup>C pulse length was 6  $\mu$ s and a recycle delay of 10 s was used.

High temperature NMR measurements were performed with a high power CP-probe. At 180°C, a maximum <sup>13</sup>C-*T*<sub>1</sub> of ~10 s was measured with a saturation recovery experiment [15] on TPV-1. <sup>13</sup>C NMR spectra were recorded at 180°C with a single excitation pulse of 6  $\mu$ s, a recycle delay of 50 s and inverse gated proton decoupling to allow for nearly complete relaxation of the nuclei between scans. In addition to the Bloch-decay experiments, Distortionless Enhanced Polarization Transfer (DEPT) was used [16].

For the <sup>13</sup>C DEPT NMR measurements, the  $\tau$ -delay was set at 4 ms, this corresponds with optimal transfer for a *J*<sub>CH</sub>-coupling of 125 Hz, which is a characteristic for aliphatic structures. The flip angle of the final proton pulse was set to 45°. The recycle delay for the <sup>13</sup>C DEPT NMR measurements was set at 20 s for the 1D measurements and at 2 s for the 2D <sup>13</sup>C-<sup>1</sup>H DEPT NMR measurement [17]. <sup>13</sup>C-*T*<sub>2</sub> relaxation experiments were performed using a Carr–Purcell/Meiboom–Gill (CP/MG) pulse sequence [18]. The interval between the 180° <sup>13</sup>C pulses was set to 250  $\mu$ s. The pulse delay was set to 20 s, which roughly corresponds to twice the longest <sup>13</sup>C-*T*<sub>1</sub>.

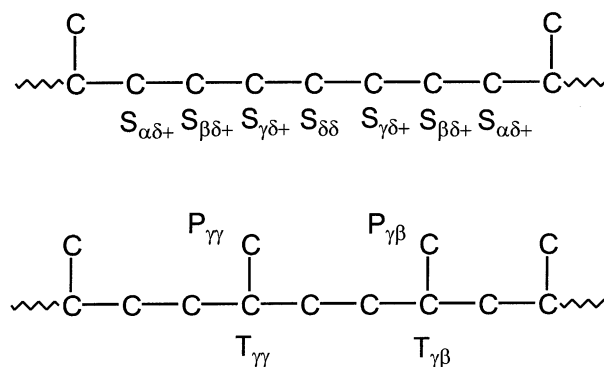
NMR spectra with a long repetition time of 50 s between scans were deconvoluted using a home-made fitting program [19]. The spectra were treated as a superposition of the spectra of each constituent using Lorentzian lines to determine the relative weight fractions. This fitting program was based on the CERN (Geneva, Switzerland) Minuit fitting package. The dataset collected from TPV-1 was first deconvoluted and the integrated intensities, the line widths and the chemical shifts of the various signals were determined. Subsequently, the other spectra were analyzed for each signal, while keeping the chemical shifts fixed to their values. This leaves the integrated intensities and the line widths of the signals as the only free parameters.

EPR was performed at room temperature using a Jeol JES-Re2x spectrometer with a Jeol Esprit 330 data system. The magnetic field was 330 mT and the transmitter frequency was set to 9.42 GHz.

### 3. Results

#### 3.1. Assignment of signals

The solution  $^{13}\text{C}$  NMR spectrum of isotactic PP in  $\text{C}_2\text{D}_2\text{Cl}_4$  is shown in Fig. 1(A). The highly site- and stereo-specific catalysis used in the preparation of PP yields a well-defined chemical structure with only head-to-tail linking of the propylene monomers and a high degree of isotacticity (mmmm pentade >93%). The  $^{13}\text{C}$  NMR spectrum of PP shows three signals, one for every carbon in the repeating monomeric unit. The methylene carbon resonates with  $\delta = 46.1$  ppm, while the methine and methyl carbons resonate with  $\delta = 28.5$  ppm and  $\delta = 21.6$  ppm, respectively [20]. The  $^{13}\text{C}$  response of the molten PP is shifted downfield compared to the response from the same sample measured with liquid NMR at  $120^\circ\text{C}$  in  $\text{C}_2\text{D}_2\text{Cl}_4$ . The high-temperature chemical shifts, at  $180^\circ\text{C}$ , are 46.9, 29.2 and 22.0 ppm, for the methylene, the methine and the methyl carbon, respectively. It is possible that these small differences are related to magnetic susceptibility effects or a small temperature dependence of the chemical shifts. The solution  $^{13}\text{C}$  NMR spectrum of EPDM is shown in Fig. 1(B). Peak assignments were made by comparison with spectra reported by Carmen et al. and Randall [21,22]. EPDM comprises three different monomer units, i.e. ethylene,



Scheme 1.

propylene, and ENB, which are polymerized in a variety of sequence distributions and the corresponding  $^{13}\text{C}$  NMR spectrum is considerably more complex than the PP spectrum. In addition, the catalysis used to polymerize EPDM is non-stereo specific. As a result, the final ethylene-propylene copolymer is heterogeneous in terms of its constituting chemical structures and the  $^{13}\text{C}$  NMR spectra contain many signals. Two characteristic structural examples of EPDM, which represents  $\sim 10\%$  of the material, are depicted in Scheme 1. The response around a  $^{13}\text{C}$  chemical shift of 45–48 ppm corresponding to the methylene unit of PP is weak. The propylene units, therefore, largely occur as single isolated units. The chemical structure of the propylene fractions depends on the catalyst used and on the amount of propylene used during polymerization. The amount of third monomer, in this case ENB, is too low to produce any substantial signal intensity in the  $^{13}\text{C}$  NMR spectrum.

In the assignments depicted in Fig. 1(B), a methylene carbon is identified as S with two Greek indices indicating its distance in both directions from the nearest tertiary carbons. For instance, the letter  $\delta$  indicates that a methylene is in the  $\delta$  position relative to a tertiary carbon. Similarly, methine and methyl carbons are identified as T and P, respectively, with two Greek letters showing the positions of the nearest tertiary carbons.

The extender oil used in the TPVs is best characterized as a low molecular weight EPM oil for several reasons. The aliphatic region of the  $^{13}\text{C}$  NMR spectrum of the oil is similar to the spectrum of EPDM rubber (Fig. 1(C)). The strongest signals are at 14.0, 20.0, 22.8, 27.7, 29.9 and 37.7 ppm. The signals at 14.0, 22.8 and 32.1 ppm can be assigned to the response from the butyl chain-ends of the oil and are not observed in the  $^{13}\text{C}$  NMR spectrum of EPDM due to its high molecular weight. These signals are well separated from the response of the main EPM chain [23]. In addition, from the  $^{13}\text{C}$  NMR spectrum the number average molecular weight ( $\bar{M}_n$ ) and the ethylene contents ( $f_e$ ) of the oil were determined as  $\bar{M}_n = 800$  g/mol and  $f_e = 70$  wt%. Since there are no significant signals in the 100–160 ppm region of the  $^{13}\text{C}$  NMR spectrum of the oil, the

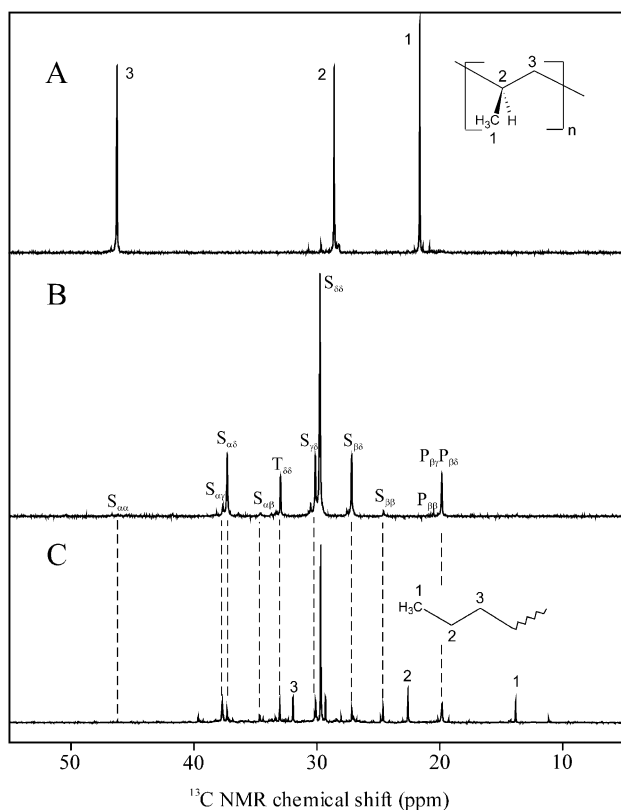


Fig. 1. Proton-decoupled  $^{13}\text{C}$  NMR spectra of PP (A), EPDM (B) and extender oil (C). All materials were dissolved in  $\text{C}_2\text{D}_2\text{Cl}_4$  and measured at  $100^\circ\text{C}$ .

relative amount of aromatics and naphthenics in the oil is very low (<1 mol%).

The technical data sheet of the extender oil, provided by the manufacturer, lists two different values; 13.7 wt% (Clay–Gel analysis) [24] and 32.0 wt% (Carbon-Type analysis) [25] for the aromatic content. Both the analytical methods are indirect methods in determining the aromatics fraction. In the case of the Clay–Gel analysis, the aromatics fraction is calculated from the amount of material that adheres to a clay adsorbent. This test method calculates the aromatics content as follows; if an aromatic ring is attached to a long saturated EPM-chain, the total chain is taken as an aromatic structure and not the separate aromatic rings alone. In the case of the Carbon-Type analysis, the amount of aromatics and naphthenics are determined by correlating the viscosity–gravity constant and the refractivity intercept with the amount of aromatics and naphthenics [26]. This test method was developed in the 1950s and was for a long time considered the best way to distinguish between different oils. However, this analysis correlates a physical property to the chemical structure of the oil, which is again an indirect method to identify the chemical structure of oils.

### 3.2. Determination of the composition

An example of a  $^{13}\text{C}$  NMR spectrum of a TPV is given in Fig. 2(A). The resonances of the oil and the EPDM are clearly resolved. It is well known that isotactic PP has two rather immobile conformational structures at room temperature, i.e. amorphous and crystalline [1,4]. Both phases have a long  $^{13}\text{C}-T_1 > 30$  s, which makes a quantitative analysis with NMR impractical. When a TPV is heated to  $180^\circ\text{C}$ , the PP is molten. At this temperature, the PP has three distinct resonances at 46.9, 29.2 and 22.0 ppm, for the methylene, the methine and the methyl carbon, respectively (Fig. 2(B)) and the  $^{13}\text{C}-T_1$  is much lower,  $\sim 2$  s.

In order to determine the distribution of oil over the two polymer phases, i.e. PP and EPDM, a quantitative NMR analysis procedure is implemented. NMR spectra with a long repetition time of 50 s between scans were deconvoluted using a home-made fitting program. The spectra were treated as a superposition of the spectra of each constituent using Lorentzian lines to determine the relative weight fractions  $m_{\text{PP}}$ ,  $m_{\text{EPDM}}$  and  $m_{\text{oil}}$  of the PP, EPDM and oil components in the TPV system, normalized according to

$$m_{\text{PP}} + m_{\text{EPDM}} + m_{\text{oil}} = 100 \quad (1)$$

Examples of such deconvoluted  $^{13}\text{C}$  NMR spectra are shown in Fig. 3(A). The three components PP, EPDM and oil are all polyolefins with approximately the same ratio H : C  $\approx 2 : 1$  and the integrated  $^{13}\text{C}$  NMR response is to a good approximation proportional to the weight percentage of each component  $m_x$ . First,  $I_{\text{total}}$  is defined as the intensity of the total  $^{13}\text{C}$  NMR response, integrated over the entire spectrum. The PP and oil components have at least one

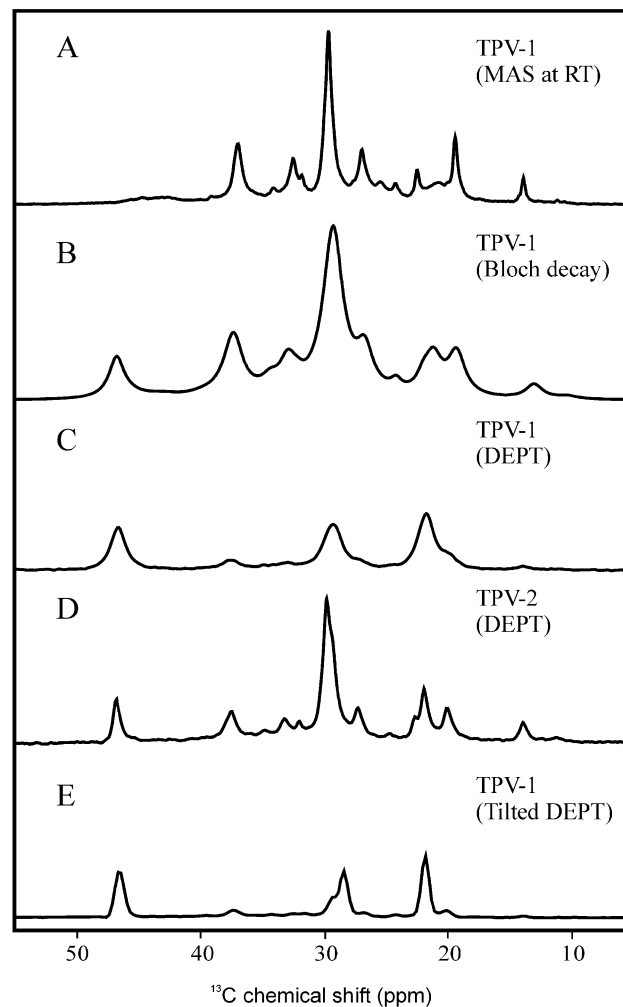


Fig. 2. Proton-decoupled  $^{13}\text{C}$  NMR MAS spectrum of TPV-1 (A). Proton-decoupled  $^{13}\text{C}$  NMR spectrum of TPV-1 at  $180^\circ\text{C}$  (B).  $^{13}\text{C}$  DEPT NMR spectra of TPV-1 and TPV-2 at  $180^\circ\text{C}$  (C and D, respectively). The response of the oil in spectrum (C) is much less than in spectrum (D) due to the presence of talcum. Projection of the  $^{13}\text{C}$  DEPT NMR data of TPV-1 shown in Fig. 5(B) (E). The spectra (B–E) were collected on static samples.

resonance that can be fully resolved with the deconvolution procedure. For the PP, the signal from the 3- $^{13}\text{C}$  methine carbon was chosen. Its intensity is denoted by  $I_{\text{PP}}^{46.7}$ . To keep track of the oil fraction, the 1- $^{13}\text{C}$  end methyl signal is used, with intensity  $I_{\text{oil}}^{14.0}$ . The EPDM signals overlap with the response from the oil, and we use the combined response of EPDM and oil at  $\delta = 20.0$  ppm with the intensity  $I_{\text{oil}}^{20.0} + I_{\text{EPDM}}^{20.0}$  to determine the EPDM fraction.

From a  $^{13}\text{C}$  NMR spectrum of the oil (Fig. 1(C)), collected with a long pulse delay of  $50 \text{ s} \gg T_1$  and inverse gated decoupling, the ratios between the individual integrals of each resonance in the  $^{13}\text{C}$  NMR spectrum of the oil can be measured from the peak intensities. The intensity ratio for the resonances at 20.0 and 14.0 ppm is

$$\frac{I_{\text{oil}}^{20.0}}{I_{\text{oil}}^{14.0}} = 1.21 \quad (2)$$

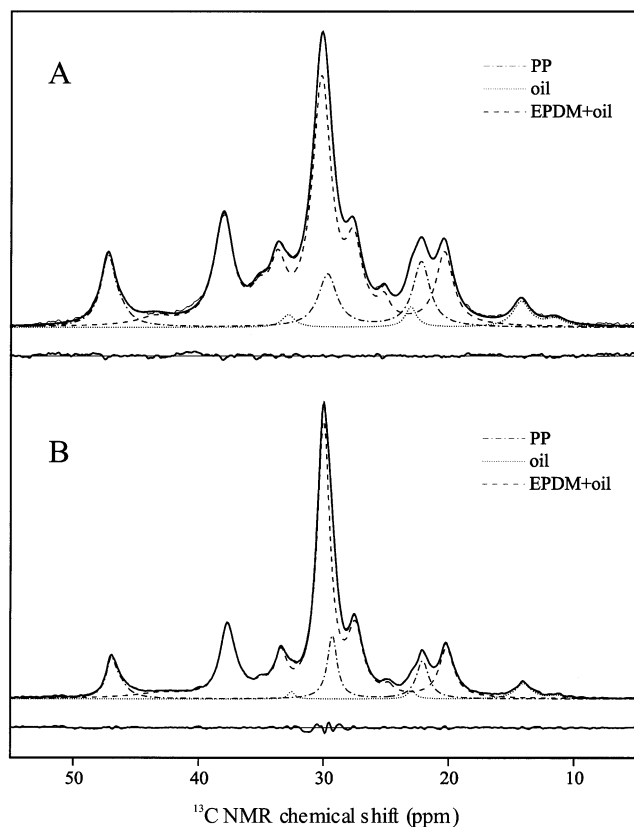


Fig. 3. Proton-decoupled  $^{13}\text{C}$  NMR spectra of TPV-1 (A) and TPV-2 (B). Data were collected on static samples at  $180^\circ\text{C}$ .

The ratio of 1.21 shows that the resonance at 20 ppm is not only due to the endgroups, but also comprises signals from the methyl resonances of the propylene units in the short polymer chain. Since PP produces three different resonances of approximately equal intensity in the  $^{13}\text{C}$  NMR spectrum (Fig. 1(A)), the percent weight fraction of PP in the material is

$$m_{\text{PP}} = \frac{3I_{\text{PP}}^{46.7}}{I_{\text{total}}} \times 100 \quad (3)$$

Since both oil and EPDM have a resonance at 20.0 ppm, the ratio of  $m_{\text{oil}}$  over  $m_{\text{oil}} + m_{\text{EPDM}}$  in the TPV can be expressed as

$$\frac{m_{\text{oil}}}{m_{\text{oil}} + m_{\text{EPDM}}} = \frac{I_{\text{oil}}^{20.0}}{I_{\text{oil}}^{20.0} + I_{\text{EPDM}}^{20.0}} \quad (4)$$

Using Eqs. (1) and (2), the oil weight fraction in the TPV is then expressed as

$$m_{\text{oil}} = (100 - m_{\text{PP}}) \frac{1.21I_{\text{oil}}^{14.0}}{I_{\text{oil}}^{20.0} + I_{\text{EPDM}}^{20.0}} \quad (5)$$

Once  $m_{\text{oil}}$  and  $m_{\text{PP}}$  are known,  $m_{\text{EPDM}}$  can easily be calculated using Eq. (1). Using this procedure, a composition analysis for the four TPVs was performed and the results summarized in Table 1.

To obtain additional information about the oil in the molten TPV-1 and TPV-2 that were prepared with and without filler, DEPT spectra were acquired (Figs. 2(C) and 3(D)). The DEPT technique explores the heteronuclear scalar  $J$ -coupling of  $\sim 125$  Hz between  $^{13}\text{C}$  and  $^1\text{H}$  to transfer magnetization from  $^1\text{H}$  to  $^{13}\text{C}$  nuclei. The DEPT technique selects mobile fractions via the small  $J$ -coupling of  $\sim 125$  Hz and a long  $T_2$ , while the signals from components with strong  $^1\text{H}$ – $^{13}\text{C}$  dipolar couplings and shorter  $T_2$  are attenuated. Any oil present in the molten PP should be very mobile at temperatures above  $160^\circ\text{C}$  and be selectively excited by the DEPT sequence.

The  $^{13}\text{C}$  DEPT NMR spectra at  $180^\circ\text{C}$  of TPV-1 and TPV-2 are shown in Fig. 2(C) and (D), respectively. The data are scaled in such a way that the intensities of the PP response at 46.7 ppm are the same in the spectra B–E. Despite the high mobility in the material, the signals from the oil in the  $^{13}\text{C}$  DEPT NMR spectrum of the TPV-1 are very weak. The  $^{13}\text{C}$  DEPT NMR of the TPV-2 provides a substantially different picture. The lines are much narrower and the response of the oil in this spectrum is very strong. This is remarkable, since the relative amounts of oil in TPV-1 and TPV-2 are comparable (Table 1).

In order to resolve the  $^{13}\text{C}$  DEPT NMR spectrum of TPV-1 in more detail, a 2D-DEPT NMR dataset was collected from TPV-1 (Fig. 4(A)). The 2D-DEPT

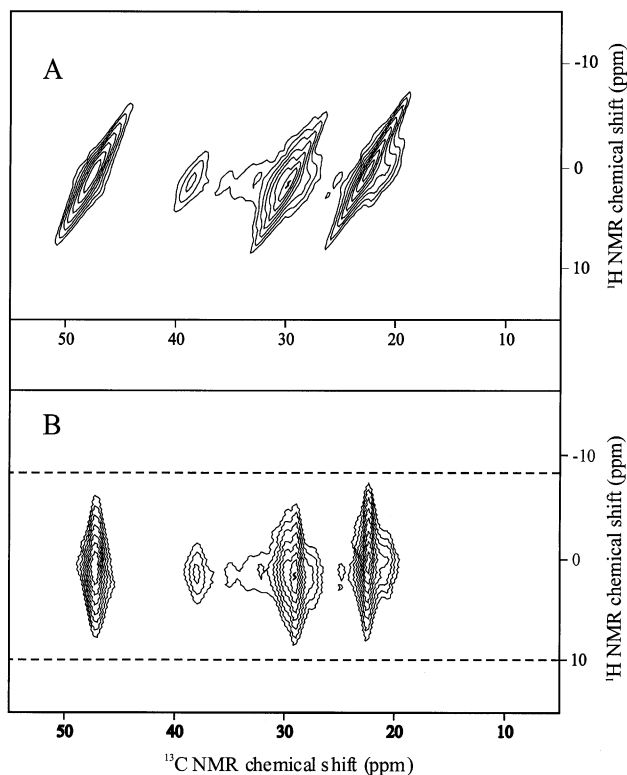


Fig. 4. 2D  $^{13}\text{C}$  DEPT NMR spectra of TPV-1 (A). The spectra were collected on a static sample at  $180^\circ\text{C}$ . The resolution of the  $^{13}\text{C}$  DEPT NMR spectrum can be enhanced by the tilting the spectrum (B). The dashed lines indicate the region that was used to obtain the partial projection shown in Fig. 3(E).

Table 2  
 $^{13}\text{C}$ - $T_2$  relaxation times of the TPV-1 and TPV-2

Chemical shift (ppm)	Carbon type + compound	$^{13}\text{C}$ - $T_2$ time (ms) TPV-1	$^{13}\text{C}$ - $T_2$ time (ms) TPV-2
46.7	$\text{CH}_2/\text{i-PP}$	$150 \pm 18$	$110 \pm 7$
37.7	$\text{CH}_2/\text{EPDM} + \text{oil}$	$120 \pm 34$	$80 \pm 4$
34.9	$\text{CH}_2/\text{EPDM} + \text{oil}$	$83 \pm 23$	$109 \pm 7$
33.3	$\text{CH}/\text{EPDM} + \text{oil}$	$151 \pm 16$	$101 \pm 7$
29.9	$\text{CH}_2/\text{EPDM} + \text{oil}$	$137 \pm 11$	$72 \pm 6$
29.3	$\text{CH}/\text{i-PP}$	$143 \pm 58$	$175 \pm 14$
27.4	$\text{CH}_2/\text{EPDM} + \text{oil}$	$108 \pm 14$	$89 \pm 7$
22.8	$\text{CH}_2/\text{oil}$	$96 \pm 16$	$237 \pm 36$
22.0	$\text{CH}_3/\text{i-PP}$	$280 \pm 62$	$165 \pm 9$
20.1	$\text{CH}_3/\text{EPDM} + \text{oil}$	$171 \pm 15$	$129 \pm 8$
14.0	$\text{CH}_3/\text{oil}$	$98 \pm 43$	$175 \pm 14$

NMR spectrum (Fig. 4(B)) was tilted and a partial projection was made of the spectral density between  $-8$  and  $10$  ppm in the  $^1\text{H}$  dimension, as indicated with dashed lines in Fig. 4(B). This projection is shown in Fig. 2(E). The resolution is much improved with respect to the  $^{13}\text{C}$  DEPT spectrum in Fig. 2(C) and is comparable with the resolution of the  $^{13}\text{C}$  DEPT spectrum of TPV-2 in Fig. 2(D).

In addition, an effort has been made to determine the  $^{13}\text{C}$ - $T_2$ -relaxation behavior of the separate components at  $180^\circ\text{C}$  in order to investigate whether the different components have the same or different relaxation behavior. This will give additional insight into the morphology of the TPV system at these high temperatures. The  $T_2$  was measured with the CP/MG pulse sequence. The results are summarized in Table 2.

Finally, EPR was performed on all four TPVs. Fig. 5 gives the EPR spectrum of TPV-1. The strong signal at  $g = 2.0036$  is due to the reference, diphenylpicrylhydrazyl (DPPH). The sextuplet corresponds to the five unpaired electrons in  $\text{Mn}^{2+}$ . These EPR measurements reveal the presence of some  $\text{MnO}$  in TPV-1, which is due to  $\text{Mn}^{2+}$  in the talcum filler. In contrast, the EPR response of TPV-2 without talcum filler is negligible.

#### 4. Discussion

The quantitative NMR analysis of the composition is listed in Table 1 for the four TPVs. For TPV-1 and TPV-3, the composition as measured by NMR is quite different from the specifications, while for TPV-2 and TPV-4 the results from the NMR analysis correspond with the recipe within experimental error. TPV-1 and TPV-3 contain talcum and the measurements indicate that about one third of the oil in TPV-1 is not detected by  $^{13}\text{C}$  NMR. In contrast, the PP/EPDM ratios calculated from the NMR data are in agreement with the specifications for all TPVs. This strongly suggests a partial suppression of the oil signal in TPVs containing talcum, which can be attributed to the

$\text{Mn}^{2+}$  paramagnetic impurities in the filler that are detected with EPR. Paramagnetic impurities like metal ions and radicals can broaden the NMR lines beyond detection by shortening the  $T_2$  to such an extent that lines disappear in the noise [27,28]. In particular,  $\text{Mn}^{2+}$  ions can induce severe line broadening of  $10^3$ – $10^4$  Hz [28]. In addition, the talcum particles will give rise to heterogeneity in the permanent magnetic field, due to differences in magnetic susceptibility in the material, which can only partly be reduced by MAS

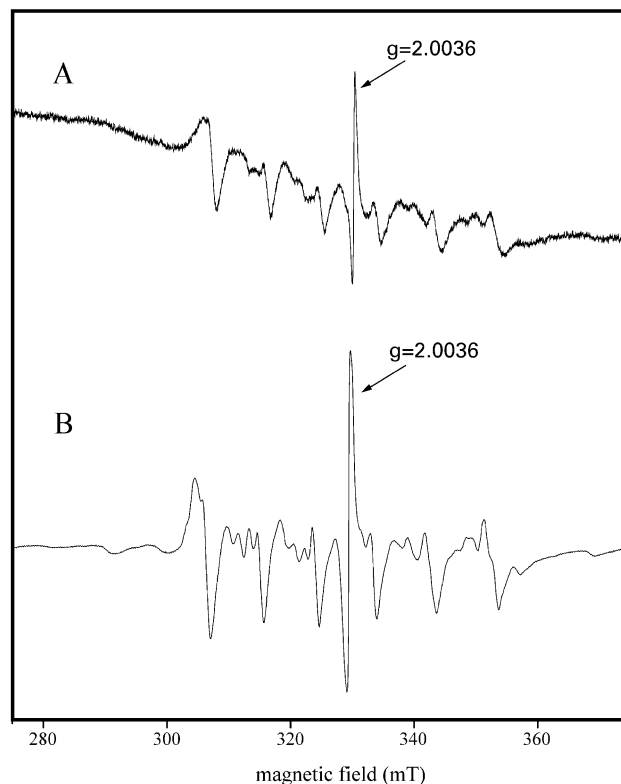


Fig. 5. ESR spectrum of TPV-1 (A) and pure talcum (B). Data were collected at room temperature. The large response in the center of the spectrum corresponds to the reference, diphenylpicrylhydrazyl (DPPH). The other six signals represent the multiplet from the five unpaired electrons of the  $\text{Mn}^{2+}$  ions.

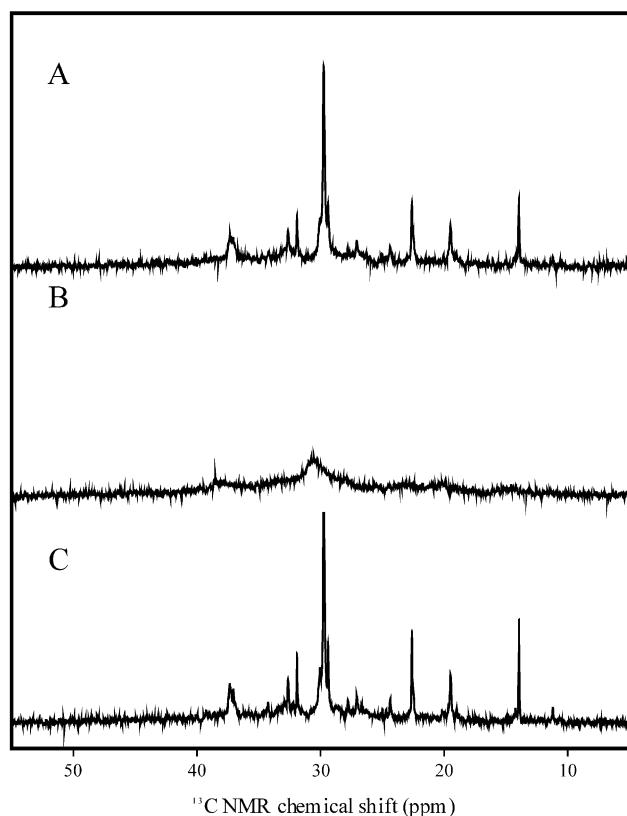


Fig. 6. Proton-decoupled  $^{13}\text{C}$  NMR spectra of pure extender oil (A), of oil mixed with talcum (B) and oil after centrifugation and separation of talcum (C). Note the difference in line width of spectrum (A) and spectrum (B).

[29,30]. This leads to the conclusion that part of the oil in contact with the filler cannot be detected by  $^{13}\text{C}$  NMR.

The pronounced effect of talcum on the  $^{13}\text{C}$  NMR signal intensity of oil can be verified with high resolution NMR. The  $^{13}\text{C}$  NMR spectrum of pure oil displays a neat spectrum with line widths of  $\sim 3$  Hz (Fig. 6(A)). When the oil is mixed with talcum to form a suspension, the lines are severely broadened (Fig. 6(B)). The oil can be separated again from the talcum particles by centrifugation. The  $^{13}\text{C}$  NMR spectrum (Fig. 6(C)) collected from the supernatant is similar to the data obtained for the pure oil (Fig. 6(A)). This supports the conclusion that in the TPV-1, part of the oil is in suspension with the filler and its NMR response is broadened beyond detection. This can also explain the weak  $^{13}\text{C}$  DEPT NMR response of the oil in TPV-1 (Fig. 2(C)). The lower resolution in the  $^{13}\text{C}$  DEPT NMR spectrum of TPV-1 compared to TPV-2 can be explained in terms of excessive inhomogeneous line broadening in TPV-1, caused by either susceptibility effects due to the finer morphology of the material or microscopic variations in bulk magnetic susceptibility in TPV-1. The homogenous line width of the PP and EPDM is marginally affected by the filler, according to Table 2 and Fig. 2(E). After shearing the 2D DEPT NMR spectrum, a substantial improvement of the resolution is obtained. Although Fig. 2(E) is comparable with Fig. 2(D), the oil signals are relatively weak compared

to the signals of the PP. Thus, the DEPT results confirm that part of the oil is suppressed by the presence of paramagnetic impurities and that the talcum perturbs the resolution of the  $^{13}\text{C}$  NMR response in TPV-1 due to additional inhomogeneous line broadening.

Both CP/MG and single pulse data collected with a spectral width of 200 kHz did not reveal broadened oil signals and a broadened oil response has a short  $^{13}\text{C}$ - $T_2 < 100$   $\mu\text{s}$  and its relaxation behavior cannot be detected by the CP/MG-pulse sequence that uses intervals of 250  $\mu\text{s}$  between the  $180^\circ$   $^{13}\text{C}$  pulses. The  $^{13}\text{C}$ - $T_2$  relaxation behavior of the remaining part of the NMR response in TPV-1 is globally the same as for TPV-2. However, the errors of some numbers in Table 2 are somewhat large. This is completely caused by the random scatter in the curve. The combined responses of EPDM and oil yield quite long  $^{13}\text{C}$ - $T_2$  relaxation times of the order of 100 ms. The  $^{13}\text{C}$ - $T_2$  relaxation of the PP in the two samples is very similar. For the  $^{13}\text{C}$ - $T_2$  relaxation of the resolved oil signals at 14.0 and 22.8 ppm, there is a minor significant difference. The relaxation times of the oil in the TPV-1 are shorter ( $^{13}\text{C}$ - $T_2 \sim 100$  ms) than for TPV-2 ( $^{13}\text{C}$ - $T_2 \sim 200$  ms). Crosslinking is thought to shorten the  $^{13}\text{C}$ - $T_2$  of the oil and the crosslink density of the EPDM in TPV-1 may be somewhat different from the crosslink density in TPV-2. This would also explain the strong  $^{13}\text{C}$  DEPT NMR response of the oil and the EPDM in TPV-2 (Fig. 2(C)), since the DEPT sequence selectively excites mobile fractions. There is no evidence that the  $\text{Mn}^{2+}$  ions present in the talcum or a difference in magnetic susceptibility enhances the  $^{13}\text{C}$ - $T_2$  relaxation of the components that can be detected by the NMR. The DEPT and  $^{13}\text{C}$ - $T_2$  measurements performed on TPV-2 give no conclusive evidence regarding the location of the oil contrary to the results presented on the location of the oil in TPV-1.

The NMR/EPR measurements reveal that at  $180^\circ\text{C}$ , the talcum particles are suspended in the oil. Apparently, the oil/filler suspension is not mixed at a molecular level with the molten PP or EPDM. The talcum does not significantly affect the NMR measurement of the PP/EPDM ratio, since the value calculated from the NMR value corresponds with the specifications within the experimental error (Table 1). If the talcum were in direct contact with either PP or EPDM, the ratio PP/EPDM measured with NMR would be different from the specifications, unless talcum would be evenly distributed over both PP and EPDM.

The talcum/oil suspension is depicted schematically in Fig. 7. The talcum particles have a rectangular shape with a length of  $\sim 3$   $\mu\text{m}$  and a width and height of  $\sim 0.1$   $\mu\text{m}$ .<sup>1</sup> The total amount of talcum in TPV-1 is 10 wt% of the material and  $0.30 \times 43 = 13$  wt% of the material represents the oil that is associated with the talcum. The specific gravity of talcum and oil are 2.8 and 0.9 g/ml, respectively. Thus, the

<sup>1</sup> This was observed in a separate study with transmission electron microscope (TEM).



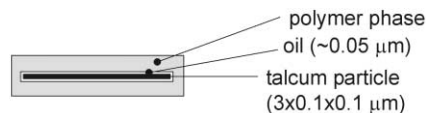


Fig. 7. Schematic representation of the characteristic TPV morphology in the melt as determined with NMR. The talcum particles are suspended in oil, and dispersed in the polymer phase.

volume ratio between oil and talcum is  $(13/10) \times (2.8/0.9) = 4.0$ . The volume of a talcum particle is  $3 \times 0.1 \times 0.1 = 0.03 \mu\text{m}^3$  and the oil volume associated with such a talcum particle is typically  $0.12 \mu\text{m}^3$ . If the rectangular talcum particle is surrounded by a thin oil film, its thickness will be on an average  $\sim 0.05 \mu\text{m}$ .

An oil layer of  $\sim 0.05 \mu\text{m}$  was not detected by TEM although this might be due to difficulties in selectively visualizing the oil. It is thus concluded that part of the oil forms a separate phase together with the talcum particles at temperatures above the melting point of PP. This is different from the morphology at room temperature, where most of the oil is probably confined in the crosslinked EPDM phase. These results confirm the assumption that the oil is not restricted to the EPDM phase at processing conditions. Upon melting, it diffuses out of the EPDM and forms a separate oil/talcum phase. This effect is important, since it may well contribute to lowering the viscosity at processing temperatures.

## 5. Conclusions

The extender oil has been characterized with  $^{13}\text{C}$  NMR. The fraction of aromatic rings or any other unsaturated carbons is very small. The oil may be considered as a low molecular weight EPM with  $\bar{M}_n = 800 \text{ g/mol}$  and an ethylene content of 70 wt%. The composition of a PP/EPDM/oil based TPV can be quantitatively determined with  $^{13}\text{C}$  NMR via spectral deconvolution. When the TPV contains talcum, the apparent relative amount of oil in the TPV as measured with NMR is too small. The talcum used as filler contains paramagnetic  $\text{Mn}^{2+}$  ions, which affect considerably the  $^{13}\text{C}$ - $T_2$  NMR relaxation of a substantial fraction of the oil in the TPV. Thirty per cent of the oil could not be detected with  $^{13}\text{C}$  NMR when talcum is present in the material. The  $\text{Mn}^{2+}$  ions appear to be associated with a separate oil phase, probably an oil/talcum suspension. The remainder of the oil is probably mixed with EPDM, since the  $^{13}\text{C}$ - $T_2$  values of the oil and the EPDM are very similar and only a small amount of oil in TPV-1 can be detected by  $^{13}\text{C}$  DEPT NMR. The presence of this oil/talcum separate phase at  $180^\circ\text{C}$  might lower the processing viscosity.

## Acknowledgements

The authors would like to thank C. Erkelens, F. Lefeber and J. Hollander at the Leiden Institute of Chemistry for the technical assistance during the NMR experiments.

## References

- [1] Coran AY. In: Bhowmick AK, Stephans HL, editors. Handbook of elastomers — new developments and technology. New York: Marcel Dekker, 1988.
- [2] Coran AY, Patel P. Rubber Chem Technol 1980;53:141.
- [3] van Duin M, Souphanthong A. Rubber Chem Technol 1995;68:717.
- [4] Coran AY. In: Legge NR, Holden G, Schroeder HE, editors. Thermoplastic elastomers — a comprehensive review. New York: Hanser Publishers, 1992.
- [5] Ellul MD. Rubber Chem Technol 1998;71:244.
- [6] Kikuchi Y, Fukui T, Okada T, Inoue T. J Appl Polym Sci: Appl Polym Symp 1992;50:261.
- [7] Kawabata S, Kitawaki S, Arisawa H, Yamashita Y, Guo X. J Appl Polym Sci: Appl Polym Symp 1992;50:245.
- [8] Gessler AM, Kresge EN. (To Advanced Elastomer Systems, L.P.), US Patent. 1979; 4, 132: 698.
- [9] Cheung TTP. Phys Rev B 1981;23:1404.
- [10] Schmidt-Rohr K, Clauss J, Blumich B, Spiess HW. Magn Reson Chem 1990;28:s3.
- [11] White JL, Mirau P. Macromolecules 1993;26:3049.
- [12] Cho G. Can J Chem 1994;72:2255.
- [13] Kimura T, Neki K, Tamura N, Horii F, Nakagawa M, Odani H. Polymer 1992;33:493.
- [14] Kulik AS, Haverkamp J. Polymer 1995;36:427.
- [15] Mc Donald GC, Leigh JS. J Magn Reson 1973;9:358.
- [16] Doddrell D, Pegg PT, Bendall MR. J Magn Reson 1982;48:323.
- [17] Levitt MH, Sørensen OW, Ernst RR. Chem Phys Lett 1983;94:540.
- [18] Rubenstein DL, Fan S, Nakashima TT. J Magn Reson 1985;64:541.
- [19] de Groot HJM, Smith SO, Kolbert AC, Courtin JMC, Winkel C, Lugtenburg J, Herzfeld J, Griffin RG. J Magn Reson 1991;91:30.
- [20] Zambelli A, Sacchi MC, Locati P, Zannoni G. Macromolecules 1982;15:211.
- [21] Carmen CJ, Harrington CE, Wilkes CE. Macromolecules 1977;10:530.
- [22] Randall JC. Macromolecules 1978;11:33.
- [23] Cheng HN, Smith DA. Macromolecules 1986;19:2065.
- [24] ASTM D2007-91: Standard test method for characteristic groups in rubber extender and processing oils and other petroleum-derived oils by the clay-gel adsorption chromatographic method. In: The Annual Book of ASTM Standards.
- [25] ASTM D2140-91: Standard test method for carbon-type composition of insulating oils of petroleum origin. In: The Annual Book of ASTM Standards.
- [26] Kurtz SS, King RW, Stout WJ, Partikian DG, Skrabek EA. Anal Chem 1956;28:1928.
- [27] Wong S, Zax DB. Electrochem Acta 1997;42:3513.
- [28] Bertini I, Turano P, Vila AJ. Chem Rev 1993;93:2833.
- [29] Kentgens APM, Veeman WS, van Bree J. Macromolecules 1987;20:1234.
- [30] Cashell EM, Douglass DC, McBrierty VJ. Polym J 1978;10:557.